Business Cycle Synchronization Across the Euro Area: a Wavelet Analysis[*]

Luís Aguiar-Conraria[†]   Maria Joana Soares[‡]

February 28, 2009

Abstract

We use wavelets, cross-wavelets, wavelet-phase analysis, wavelet-clustering and multidimensional mapping to study business cycle synchronization across countries that are part of the Euro12 Area. Based on the wavelet spectra, we propose a metric to measure business cycle disynchronicity. We identify Germany, France, Spain, Austria and the Benelux countries as the core of the Euroland and another group with a less synchronous business cycle and ask whether these latter countries are converging to the Euroland core, and, if so, at what frequencies. With the exception of Portugal, all countries are converging to the Euro core. This convergence is particularly strong in the case of Ireland and Italy.

Keywords: Business Cycle Synchronization, Continuous Wavelet Transform, Wavelet Coherency, Phase-Difference, Wavelet Spectra Distance Matrix, Clustering Analysis, Multidimensional Scaling

[†]NIPE and Economics Departament, University of Minho, E-mail address: lfaguiar@eeg.uminho.pt
[‡]Mathematics Departament, University of Minho, E-mail address: jsoares@math.uminho.pt

1

1 Introduction

The business cycle synchronization literature is related to the literature on optimal currency areas and, more broadly, on economic unions. The idea is simple. If several countries delegate on some supranational institution the power to perform a common monetary (or fiscal) policy, then they loose this policy stabilization instrument. If countries have asymmetric business cycles then it may not be optimal to have the same decision applied to every country. Naturally, business cycle synchronization is not sufficient to guarantee that a monetary union is desirable. But it is a necessary condition. Therefore, a country with an asynchronous business cycle faces several difficulties in a monetary union, because of the 'wrong' stabilization policies. With the recent enlargement of the European Union, the interest on this topic is guaranteed for a while.

The literature on business cycle comovements is large, and growing, and may be subdivided in several branches, which are not isolated between themselves. One branch is concerned about the best way to estimate a common business cycle. For example, the EuroCOIN, a coincident indicator that measures European Economic Activity is based on the work of Forni *et al.* (2000), who rely on a dynamic factor model to extract the common European Activity Index. Another example of this type of approach is given by Artis *et al.* (2004) that uses Markov switching autoregressions and Markov switching vector-autoregressions to identify a common unobserved component that determines an European business cycle dynamics. Another branch tries to answer the question of whether there is a common business cycle or not. For example, Camacho *et al.* (2006) and Harding and Pagan (2006) discuss how the degree of synchronization between business cycles of different countries can be measured and tested. The empirical evidence on the existence of an European business cycle is mixed. Clark and Wincoop (2001) document that business cycles of U.S. Census regions are substantially more synchronized than those of European countries and Camacho *et al.* (2006) conclude that there is no common business cycle across Europe, while Artis *et al.* (2004) find a common component governing European business cycle dynamics. Finally, some authors are concerned with the determinants of business cycle comovements.

Selover and Jensen (1999) take a purely mathematical modeling approach to conclude that the world business cycle may result from a mode-locking phenomenon (a nonlinear process by which weak coupling between oscillating systems tends to synchronize oscillations in the systems). Most other authors look for economic reasons. Frankel and Rose (1998) focus on the effects of international trade and Rose and Engel (2002) argue that, because currency union members have more trade, business cycles are more synchronized across currency union countries. According to Imbs (2004), economic regions with strong financial links are significantly more synchronized. Particularly relevant to our analysis are the results of Inklaar *et al.* (2008), who conclude that convergence in monetary and fiscal policies have a significant impact on business cycle synchronization. Again, evidence on this topic is mixed. Baxter and Kouparitsas (2005), for example, argue that currency unions are not important determinants of business cycle synchronization (or at least this effect is not robust) and Camacho *et al.* (2008) present evidence that differences between business cycles in Europe have not been disappearing.

We argue that wavelet analysis is particularly well-suited to study business cycle synchronism. With the wavelet transform, we estimate the evolution of the power spectrum across time. We propose a metric to compare the power spectra. With that metric, we fill a dissimilarity matrix, which is used, with clustering techniques and multidimensional scaling, to group the countries in terms of business cycle synchronism. Then, using cross-wavelets, wavelet-phase and phase difference analysis, we are able to study when and at what frequencies did that synchronization start. We focus on the first countries that joined the Euro (plus Greece). We identify a group of countries that form the core of the Euroland in terms of business cycle synchronism: Germany, France, Austria, Spain and the Benelux countries. The group with the least synchronous cycles is formed by Portugal, Italy, Greece and Finland. It is not clear in which of the groups we should include Ireland. We also conclude that, with the exception of Portugal, all countries in the asynchronous group are converging to the Euro core. This convergence is particularly strong in the case of Ireland and Italy.

The paper proceeds as follows. In section 2, we discuss the main advantages of wavelet analysis, its applications to economics and some of the typical difficulties in applying it to study economic relations. We present the continuous wavelet transform, discuss its localization properties and the optimal characteristics of the Morlet wavelet. We also describe the wavelet power spectrum, how to measure wavelet spectra dissimilarities, the cross-wavelet power spectrum, the wavelet coherency and the phase-difference. In section 3, we apply these tools to study business cycle synchronism across the Euro12-area. Section 4 concludes.

2 Wavelets: Frequency Analysis Across Time

Wavelet analysis performs the estimation of the spectral characteristics of a time-series as a function of time, revealing how the different periodic components of the time-series change over time. While the Fourier transform breaks down a time-series into constituent sinusoids of different frequencies and infinite duration in time, the wavelet transform expands the time-series into shifted and scaled versions of a function that has limited spectral band and limited duration in time.[1]

As a coherent mathematical body, wavelet theory was born in the mid-1980s (Grossmann and Morlet 1984, Goupillaud *et al.* 1984). The literature rapidly expanded and wavelet analysis is now extensively used in physics, epidemiology, signal processing, etc. Still, this technique is infrequently used in Economics. One peculiarity of the applications of wavelet to economics is the almost exclusive use of the discrete wavelet transform, e.g. Gençay *et al.* (2005), instead of the continuous transform that we use in this paper. To our knowledge, Raihan *et al.* (2005), Crowley *et al.* (2006) and Aguiar-Conraria *et al.* (2008) are the only exceptions to this rule. For a detailed review of wavelet applications to economic and financial data, the reader is referred to Crowley (2007).

Most of the times, these techniques have either been applied to analyze individual time-series (e.g. Gallegati and Gallegati 2007) or used to individually analyze several time-series (one each time), whose decompositions are then studied using traditional time-domain methods (e.g. Ramsey and Lampart 1998a and 1998b). However, wavelet tools have been generalized to accommodate the analysis of time-frequency dependencies between two time-series: the cross-wavelet power, the cross-wavelet coherency, and the phase-difference, proposed by Hudgins *et al.* (1993) and Torrence and Compo (1998) have been applied in different scientific fields. Gallegati (2008) — using the Maximum Overlap Discrete Wavelet Transform —, Crowley *et al.* (2006) and Aguiar-Conraria *et al.* (2008) — using the Continuous Wavelet

---

[1]We know from the Heisenberg uncertainty principle that there is always a trade-off between localization in time and localization in frequency. However, a mother wavelet can be chosen with a fast decay in time and frequency which, for all practical purposes, corresponds to an effective band and time limiting; see Daubechies (1992).

Transform — showed that cross-wavelet analysis could be fruitfully applied to study pairs of Economic time-series.

While the (single) wavelet power spectrum describes the evolution of the variance of a time-series at the different frequencies, with periods of large variance associated with periods of large power at the different scales, the cross-wavelet power of two time-series describes the local covariance between the time-series. On the other hand, one can look at the wavelet coherency as a localized correlation coefficient in the time frequency space. The phase can be viewed as the position in the pseudo-cycle of the series as a function of frequency, therefore the phase-difference gives us information on the delay, or synchronization, between oscillations of the two time-series. See Bloomfield *et al.* (2004) and Aguiar-Conraria *et al.* (2008).

To estimate a dissimilarity matrix between countries based on their wavelet spectra, one has to find a metric to measure the distances between two wavelet spectra. Comparing time-series based on their wavelet spectra is, in a sense, like comparing two images. Direct comparison is not suitable because there is no guarantee that regions of low power will not overshadow the comparison. It would be like comparing two pencil-drawing sketches based mainly on the color of the paper, disregarding the sketches themselves. We build on the work of Rouyer *et al.* (2008) and use the singular value decomposition (SVD) of a matrix to focus on the common high power time-frequency regions. This method is similar to Principal Component Analysis, but while with the latter finds linear combinations that maximize the variance, subject to some orthogonality conditions, the method we use extracts the components that maximize covariances instead, subject to similar orthogonality conditions. Therefore, the first extracted components correspond to the most important common patterns between the two wavelet spectra. With that information, and after defining a metric to measure the pairwise distance between the several extracted components, we can build a dissimilarity matrix between the several analyzed countries. From that point it is easy to implement clustering and multidimensional mapping algorithms.

2.1 The Wavelet

In what follows, $L^2(\mathbb{R})$ denotes the set of square integrable functions, i.e. the set of functions defined on the real line such that $\|x\| := \int_{-\infty}^{\infty} |x(t)|^2 \, dt < \infty$, with the usual inner product, $\langle x, y \rangle := \int_{-\infty}^{\infty} x(t) y^*(t) \, dt$. The asterisk superscript denotes complex conjugation. Given a function $x(t) \in L^2(\mathbb{R})$, $X(f) := \int_{-\infty}^{\infty} x(t) e^{-i2\pi ft} dt$ will denote the Fourier transform of $x(t)$. We recall the well-known Parseval relation, valid for all $x(t), y(t) \in L^2(\mathbb{R})$, $\langle x(t), y(t) \rangle = \langle X(f), Y(f) \rangle$, from which the Plancherel identity immediately follows: $\|x(t)\|^2 = \|X(f)\|^2$. The minimum requirements imposed on a function $\psi(t)$ to qualify for being a *mother (admissible or analyzing) wavelet* are that $\psi \in L^2(\mathbb{R})$ and also fulfills a technical condition, usually referred to as the *admissibility condition*, which reads as follows:

$$0 < C_\psi := \int_{-\infty}^{\infty} \frac{|\Psi(f)|}{|f|} df < \infty, \tag{1}$$

where $\Psi(f)$ is the Fourier transform of $\psi(t)$, see Daubechies (1992, p. 24).

The wavelet ψ is usually normalized to have unit energy: $\|\psi\|^2 = \int_{-\infty}^{\infty} |\psi(t)|^2 \, dt = 1$. The square integrability of ψ is a very mild decay condition; the wavelets used in practice have much faster decay; typical behavior will be exponential decay or even compact support. For functions with sufficient decay it turns out that the admissibility condition (1) is equivalent to requiring $\Psi(0) = \int_{-\infty}^{\infty} \psi(t) \, dt = 0$. This means that the function ψ has to wiggle up and down the $t-$axis, i.e. it must behave like a wave; this, together with the decaying property, justifies the choice of the term wavelet (originally, in French, *ondelette*) to designate ψ.

2.2 The Continuous Wavelet Transform

Starting with a mother wavelet ψ, a family $\psi_{s,\tau}$ of "wavelet daughters" can be obtained by simply scaling ψ by s and translating it by τ

$$\psi_{s,\tau}(t) := \frac{1}{\sqrt{|s|}} \psi\left(\frac{t-\tau}{s}\right), \quad s, \tau \in \mathbb{R}, s \neq 0. \tag{2}$$

The parameter s is a scaling or dilation factor that controls the length of the wavelet (the factor $1/\sqrt{|s|}$ being introduced to guarantee preservation of the unit energy, $\|\psi_{s,\tau}\| = 1$) and τ is a location parameter that indicates where the wavelet is centered. Scaling a wavelet simply means stretching it (if $|s| > 1$), or compressing it (if $|s| < 1$).[2]

Given a function $x(t) \in L^2(\mathbb{R})$ (a time-series), its continuous wavelet transform (CWT) with respect to the wavelet ψ is a function $W_x(s, \tau)$ obtained by projecting $x(t)$, in the L^2 sense, onto the over-complete family $\{\psi_{s,\tau}\}$:

$$W_x(s, \tau) = \langle x, \psi_{s,\tau} \rangle = \int_{-\infty}^{\infty} x(t) \frac{1}{\sqrt{|s|}} \psi^* \left(\frac{t - \tau}{s} \right) dt. \qquad (3)$$

Because the wavelet function $\psi(t)$ may, in general, be complex, the wavelet transform W_x may also be complex. The transform can then be divided into its real part, $\mathcal{R}\{W_x\}$, and imaginary part, $\mathcal{I}\{W_x\}$, or in its amplitude, $|W_x|$, and phase, $\phi_x(s, \tau) = \tan^{-1}\left(\frac{\mathcal{I}\{W_x\}}{\mathcal{R}\{W_x\}} \right)$. The phase of a given time-series $x(t)$ can be viewed as the position in the pseudo-cycle of the series. For real-valued wavelet functions the imaginary part is zero and the phase is undefined. Therefore, in order to separate the phase and amplitude information of a time-series it is important to make use of complex wavelets. It is also convenient to choose $\psi(t)$ to be *progressive* or *analytic*, i.e. to be such that $\Psi(f) = 0$ for $f < 0$.[3]

The importance of the admissibility condition (1) comes from the fact that it guarantees that it is possible to recover $x(t)$ from its wavelet transform. When ψ is analytic, if $x(t)$ is real,[4] the reconstruction formula is given by

$$x(t) = \frac{2}{C_\psi} \int_0^\infty \left[\int_{-\infty}^{\infty} \mathcal{R}\left(W_x(s, \tau) \psi_{s,\tau}(t) \right) d\tau \right] \frac{ds}{s^2}. \qquad (4)$$

Therefore, we can easily go from $x(t)$ to its wavelet transform, and from the wavelet transform back to $x(t)$. Note that one can limit the integration over a range of scales, performing a band-pass filtering of the original series. See Daubechies (1992, pp. 27-28) or

---

[2] Note that for negative s, the function is also reflected.

[3] Note that an analytic function is necessarily complex.

[4] See Aguiar-Conraria *et al.* (2008) for the case of complex $x(t)$.

Kaiser (1994, pp. 70-73) for more details about analytic wavelets.

2.3   Localization Properties

Let the wavelet ψ be normalized so that $\|\psi\| = 1$ and define its center μ_t by

$$\mu_t = \int_{-\infty}^{\infty} t \left| \psi(t) \right|^2 dt. \tag{5}$$

In other words, the center of the wavelet is simply the mean of the probability distribution obtained from $\left| \psi(t) \right|^2$. As a measure of concentration of ψ around its center one usually takes the standard deviation σ_t:

$$\sigma_t = \left\{ \int_{-\infty}^{\infty} (t - \mu_t)^2 \left| \psi(t) \right|^2 dt \right\}^{\frac{1}{2}}. \tag{6}$$

In a total similar manner, one can also define the center μ_f and standard deviation σ_f of the Fourier transform $\Psi(f)$ of ψ.

The interval $[\mu_t - \sigma_t, \mu_t + \sigma_t]$ is the set where ψ attains its "most significant" values whilst the interval $\left[\mu_f - \sigma_f, \mu_f + \sigma_f \right]$ plays the same role for $\Psi(f)$. The rectangle $[\mu_t - \sigma_t, \mu_t + \sigma_t] \times \left[\mu_f - \sigma_f, \mu_f + \sigma_f \right]$ in the (t, f) −plane is called the Heisenberg box or window in the time-frequency plane. We then say that ψ is localized around the point $\left(\mu_t, \mu_f \right)$ of the time-frequency plane with uncertainty given by $\sigma_t \sigma_f$. The uncertainty principle, first established by Werner Karl Heisenberg in the context of Quantum Mechanics, gives a lower bound on the product of the standard deviations of position and momentum for a system, implying that it is impossible to have a particle that has an arbitrarily well-defined position and momentum simultaneously. In our context, the Heisenberg uncertainty principle establishes that the uncertainty is bounded from below by the quantity $1/4\pi$:

$$\sigma_t \sigma_f \geq \frac{1}{4\pi}. \tag{7}$$

If the mother wavelet ψ is centered at μ_t, has standard deviation σ_t and its wavelet

transform $\Psi(f)$ is centered at μ_f with a standard deviation σ_f, then one can easily show that the daughter wavelet $\psi_{\tau,s}$ will be centered at $\tau + s\mu_t$ with standard deviation $s\sigma_t$, whilst its Fourier transform $\Psi_{s,\tau}$ will have center $\frac{\mu_f}{s}$ and standard deviation $\frac{\sigma_f}{s}$.

From the Parseval relation, we know that $W_x(s,\tau) = \langle x(t), \psi_{s,\tau}(t) \rangle = \langle X(f), \Psi_{s,\tau}(f) \rangle$. Therefore, the continuous wavelet transform $W_x(s,\tau)$ gives us local information within a time-frequency window $[\tau + s\mu_t - s\sigma_t, \tau + s\mu_t + s\sigma_t] \times [\frac{\mu_f}{s} - \frac{\sigma_f}{s}, \frac{\mu_f}{s} + \frac{\sigma_f}{s}]$. In particular, if ψ is chosen so that $\mu_t = 0$ and $\mu_f = 1$, then the window associated with $\psi_{\tau,s}$ becomes

$$\left[\tau - s\sigma_t, \tau + s\sigma_t\right] \times \left[\frac{1}{s} - \frac{\sigma_f}{s}, \frac{1}{s} + \frac{\sigma_f}{s}\right] \tag{8}$$

In this case, the wavelet transform $W_x(s,\tau)$ will give us information on $x(t)$ for t near the instant $t = \tau$, with precision $s\sigma_t$, and information about $X(f)$ for frequency values near the frequency $f = \frac{1}{s}$, with precision $\frac{\sigma_f}{s}$. Therefore, small/large values of s correspond to information about $x(t)$ in a fine/broad scale and, even with a constant area of the windows, $A = 4\sigma_t\sigma_f$, their dimensions change according to the scale; the windows stretch for large values of s (broad scales s – low frequencies $f = 1/s$) and compress for small values of s (fine scale s – high frequencies $f = 1/s$). This is one major advantages afforded by the wavelet transform, when compared to the Short Time Fourier Transform: its ability to perform natural local analysis of a time-series in the sense that the length of wavelets varies endogenously. It stretches into a long wavelet function to measure the low frequency movements; and it compresses into a short wavelet function to measure the high frequency movements.

2.4 The Morlet Wavelet: optimal joint time-frequency concentration

There are several types of wavelet functions available with different characteristics, such as, Morlet, Mexican hat, Haar, Daubechies, etc. Since the wavelet coefficients $W_x(s,\tau)$ contain combined information on both the function $x(t)$ and the analyzing wavelet $\psi(t)$,

the choice of the wavelet is an important aspect to be taken into account, which will depend on the particular application one has in mind. We choose a complex wavelet, as it yields a complex transform, with information on both the amplitude and phase, important to study the business cycle synchronism between different time-series.

We will use the Morlet wavelet, introduced in Goupillaud *et al.* (1984):

$$\psi_\eta\left(t\right) = \pi^{-\frac{1}{4}}\left(e^{i\eta t} - e^{-\frac{\eta^2}{2}}\right)e^{-\frac{t^2}{2}}. \tag{9}$$

The term $e^{-\frac{\eta^2}{2}}$ is introduced to guarantee the fulfillment of the admissibility condition; however, for $\eta \geq 5$ this term becomes negligible. The simplified version

$$\psi_\eta\left(t\right) = \pi^{-\frac{1}{4}}e^{i\eta t}e^{-\frac{t^2}{2}} \tag{10}$$

of (9) is normally used (and still referred to as a Morlet wavelet). Our results in the next section, were obtained with the particular choice $\eta = 6$.

This wavelet has interesting characteristics. First of all, it is (almost) analytic. For $\eta > 5$, for all practical purposes, the wavelet can be considered as analytic; see Foufoula-Georgiou and Kumar (1994).

The wavelet (10) is centered at the point $\left(0, \frac{\eta}{2\pi}\right)$ of the time-frequency plane; hence, for the particular choice $\eta = 6$, one has that the frequency center is $\mu_f = \frac{6}{2\pi}$ and the relationship between the scale and frequency is simply $f = \frac{\mu_f}{s}$. Therefore there is biunivocal relation between scale and frequency and we will use both terms interchangeably

It is simple to verify that the time standard deviation is $\sigma_t = 1/\sqrt{2}$ and the frequency standard deviation is $\sigma_f = 1/\left(2\pi\sqrt{2}\right)$. Therefore, the uncertainty of the corresponding Heisenberg box attains the minimum possible value $\sigma_t\sigma_f = \frac{1}{4\pi}$. In this sense, the Morlet wavelet has optimal joint time-frequency concentration.

2.5 Wavelet Power Spectrum

In view of the energy preservation formula, and in analogy with the terminology used in the Fourier case, we simply define the (local) wavelet power spectrum as $S_x(s, \tau) = |W_x(s, \tau)|^2$, which gives us a measure of the local variance. Torrence and Compo (1998), showed how the statistical significance of wavelet power can be assessed against the null hypothesis that the data generating process is given by an $AR(0)$ or $AR(1)$ stationary process with a certain background power spectrum (P_f).[5] For more general processes, one has to rely on Monte Carlo Simulations.

2.6 Cross-Wavelets and Phase-Differences

2.6.1 Cross-Wavelet Power

The cross-wavelet transform of two time-series, $x(t)$ and $y(t)$, first introduced by Hudgins *et al.* (1993), is simply defined as

$$W_{xy}(s, \tau) = W_x(s, \tau) W_y^*(s, \tau), \tag{11}$$

where W_x and W_y are the wavelet transforms of x and y, respectively. The cross-wavelet power is given by $|W_{xy}|$. While we can interpret the wavelet power spectrum as depicting the local variance of a time-series, the cross-wavelet power of two time-series depicts the local covariance between these time-series at each scale and frequency. Therefore, cross-wavelet power gives us a quantified indication of the similarity of power between two time-series. Torrence and Compo (1998) also derived the cross-wavelet distribution assuming that the two time-series have Fourier Spectra P_f^x and P_f^y.[6] For more general data generating processes one has to rely on Monte Carlo simulations.

---

[5] $D\left(\frac{|W_x(s,\tau)|^2}{\sigma_x^2} < p\right) = \frac{1}{2} P_f \chi_v^2(p)$, at each time τ and scale s. The value of P_f is the mean spectrum at the Fourier frequency f that corresponds to the wavelet scale s — in our case $s \approx \frac{1}{f}$, see equation (??) — and v is equal to 1 or 2, for real or complex wavelets respectively.

[6] Under the null, the cross-wavelet distribution is given by $D\left(\frac{|W_x W_y^*|}{\sigma_x \sigma_y} < p\right) = \frac{Z_v(p)}{v}\sqrt{P_f^x \ P_f^y}$, where $Z_v(p)$ is the confidence level associated with the probability p for a pdf defined by the square root of the product of two χ^2 distributions.

2.6.2 Wavelet Coherency

As in the Fourier spectral approaches, wavelet coherency can be defined as the ratio of the cross-spectrum to the product of the spectrum of each series, and can be thought of as the local correlation, both in time and frequency, between two time-series. The wavelet coherency between two time-series, $x(t)$ and $y(t)$, is defined as follows:

$$R_{xy}(s, \tau) = \frac{|S(W_{xy}(s, \tau))|}{|S(W_{xx}(s, \tau))|^{\frac{1}{2}} |S(W_{yy}(s, \tau))|^{\frac{1}{2}}}, \tag{12}$$

where S denotes a smoothing operator in both time and scale. Smoothing is necessary. Without that step, coherency is identically one at all scales and times. Smoothing is achieved by a convolution in time and scale. The time convolution is done with a Gaussian and the scale convolution is performed by a rectangular window; see Cazelles *et al.* (2007) for details.

Theoretical distributions for wavelet coherency have not been derived yet. Therefore, to assess the statistical significance of the estimated wavelet coherency, one has to rely on Monte Carlo simulation methods.

2.6.3 Phase Difference and the Instantaneous Time Lag

The phase-difference gives us information about the delays of the oscillations between two time-series, $x(t)$ and $y(t)$, as a function of time and frequency. As we said before, the phase of a given time-series, ϕ_x, can be viewed as the position in the pseudo-cycle of the series. The phase-difference, $\phi_{x,y}$, characterizes phase relationships between the two time-series, i.e. their relative position in the pseudo-cycle. The phase-difference is defined as

$$\phi_{x,y}(s, \tau) = \tan^{-1}\left(\frac{\mathcal{I}\{W_{xy}(s, \tau)\}}{\mathcal{R}\{W_{xy}(s, \tau)\}}\right), \quad \text{with} \quad \phi_{x,y} \in [-\pi, \pi]. \tag{13}$$

A phase-difference of zero indicates that the time-series move together at the specified frequency. If $\phi_{x,y} \in \left(0, \frac{\pi}{2}\right)$ then the series move in phase, but the time-series y leads x. If $\phi_{x,y} \in \left(-\frac{\pi}{2}, 0\right)$ then it is x that is leading. A phase-difference of π (or $-\pi$) indicates an anti-phase relation. If $\phi_{x,y} \in \left(\frac{\pi}{2}, \pi\right)$ then x is leading. Time-series y is leading if $\phi_{x,y} \in \left(-\pi, -\frac{\pi}{2}\right)$.

With the phase difference one can calculate the instantaneous time lag between the two time-series:

$$\Delta T\left(s,\tau\right) = \frac{\phi_{x,y}\left(s,\tau\right)}{2\pi F\left(\tau\right)}, \tag{14}$$

where $F\left(\tau\right)$ is the instantaneous frequency defined in a given frequency band as the first normalized moment in frequency of W_{xy}:

$$F\left(\tau\right) = \frac{\int_{f_1}^{f_2} f\left|W_{xy}\left(f,\tau\right)\right| df}{\int_{f_1}^{f_2}\left|W_{xy}\left(f,\tau\right)\right| df} \tag{15}$$

2.7 Transform of finite discrete data

If one is dealing with a discrete time-series $x = \{x_n,\ n = 0,\ldots,T-1\}$ of T observations with a uniform time step δt, the integral in (3) has to be discretized and is, therefore, replaced by a summation over the T time steps; also, it is convenient, for computational efficiency, to compute the transform for T values of the parameter τ, $\tau = m\delta t;\ m = 0,\ldots,T-1$. In practice, naturally, the wavelet transform is computed only for a selected set of scale values $s \in \{s_k, k = 0,\ldots,F-1\}$ (corresponding to a certain choice of frequencies f_k). Hence, our computed wavelet spectrum of the discrete-time series x will simply be a $F \times T$ matrix W_x whose (k,m) element is given by

$$W_x(k,m) = \frac{\delta t}{\sqrt{s_k}} \sum_{n=0}^{T-1} x_n \psi^*\left((n-m)\frac{\delta t}{s_k}\right) \quad k = 0,\ldots,F-1,\ \ m = 0,\ldots,T-1. \tag{16}$$

Although it is possible to calculate the wavelet transform using the above formula for each value of k and m, one can also identify the computation for all the values of m simultaneously as a simple convolution of two sequences; in this case, one can follow the standard procedure and calculate this convolution as a simple product in the Fourier domain, using the Fast Fourier Transform algorithm to go forth and back from time to spectral domain; this is the technique prescribed by Torrence and Compo (1998).[7]

---

[7]A program code based on the above procedure is available at the site http://paos.colorado.edu/research/wavelets/.

As with other types of transforms, the CWT applied to a finite length time-series inevitably suffers from border distortions; this is due to the fact that the values of the transform at the beginning and the end of the time-series are always incorrectly computed, in the sense that they involve "missing" values of the series which are then artificially prescribed; the most common choices are zero padding – extension of the time-series by zeros – or periodization. Since the "effective support" of the wavelet at scale s is proportional to s, these edge-effects also increase with s. The region in which the transform suffers from these edge effects is called the cone of influence. In this area of the time-frequency plane the results are unreliable and have to be interpreted carefully. In this paper, the cone of influence is defined, following Torrence and Compo (1998), as the $e-$folding time of the wavelet at the scale s, that is, so that the wavelet power of a Dirac δ at the edges decreases by a factor of e^{-2}. In the case of the Morlet wavelet this is given by $\sqrt{2}s$.

2.8 Wavelet Spectra Distance Matrix

The SVD decomposition of the covariance matrix $C_{xy} := W_x W_y^H$, where W_y^H is the conjugate transpose, also known as the Hermitian transpose, of W_y yields

$$C_{xy} = U\Sigma V^H,$$

where the matrices U and V are unitary matrices (i.e. $U^H U = V^H V = I$), whose columns, $\mathbf{u}_k$ and $\mathbf{v}_k$ are, respectively, the singular vectors for W_x and W_y, and Σ is a diagonal matrix with the singular values ordered from highest to lowest, $\sigma_1 \geq \sigma_2 \geq \ldots \geq \sigma_F \geq 0$. The number of nonzero singular values is equal to the rank of the matrix C_{xy}. The SVD of C_{xy} guarantees that the singular vectors $\mathbf{u}_k$ and $\mathbf{v}_k$ solve the problem of maximizing

$$\mathbf{p}_k^H C_{xy} \mathbf{q_k} = \mathbf{p}_k^H W_x W_y^H \mathbf{q_k} = \mathbf{p}_k^H W_x \left(\mathbf{q}_k^H W_y \right)^H$$

for all vectors $\mathbf{p}_k$ and $\mathbf{p}_k$ satisfying the orthogonality constraints $\mathbf{p}_k^H \mathbf{p}_j = \delta_{kj}$, $\mathbf{q}_k^H \mathbf{q}_j = \delta_{kj}$, $j = 1, \ldots, k$, where δ_{kj} is the Kronecker delta. In other words, the so-called *leading patterns*,

15

obtained by projecting each spectrum W_x and W_y onto the respective singular vectors,

$$L_x^k := \mathbf{u}_k^H W_x \quad \text{and} \quad L_y^k := \mathbf{v}_k^H W_y, \tag{17}$$

are the linear combinations of the columns of W_x and W_y, respectively, that maximize their mutual covariance (subject to the referred orthogonality constraints). Moreover, since $U^H W_x W_y V = U^H C_{xy} V = \Sigma$, it follows immediately that the (squared) covariance of the kth leading patterns is given by

$$|L_x^k (L_y^k)^H|^2 = \sigma_k^2.$$

On the other hand, the (squared) covariance of W_x and W_y is given by $\|C_{xy}\|_F^2$, where $\|.\|_F$ is the Frobenius matrix norm, defined by $\|A\|_F := \sqrt{\sum_{ij} |a_{ij}|^2}$. But, since this norm is invariant under a unitary transformation, we have

$$\|C_{xy}\|_F^2 = \|U^H C_{xy} V\|_F^2 = \|\Sigma\|_F^2 = \sum_{i=1}^F \sigma_i^2.$$

The (squared) singular values, σ_k^2, are the weights to be attributed to each leading pattern and are equal to the (squared) covariance explained by each pair of singular vectors (axis).

If we denote by L_x and L_y the matrices whose rows are the leading patterns L_x^k and L_y^k, equation(17) shows that $L_x = U^H W_x$ and $L_y = V^H W_y$, from where we immediately obtain

$$W_x = U L_x = \sum_{k=1}^F \mathbf{u}_k L_x^k, \qquad W_y = V L_y = \sum_{k=1}^F \mathbf{v}_k L_y^k.$$

In practice, we select a certain number $K < F$ of leading patterns, guaranteeing, for example, that the fraction of covariance $\left(\sum_{k=1}^K \sigma_k^2 \right) / \left(\sum_{k=1}^F \sigma_k^2 \right)$ is above a certain threshold, and use

$$W_x \approx \sum_{k=1}^K \mathbf{u}_k L_x^k, \quad W_y \approx \sum_{k=1}^K \mathbf{v}_k L_y^k.$$

What we have done so far is to reduce the information contained in the two wavelet spectra to a few components. Now we need to find a metric to measure the distance between
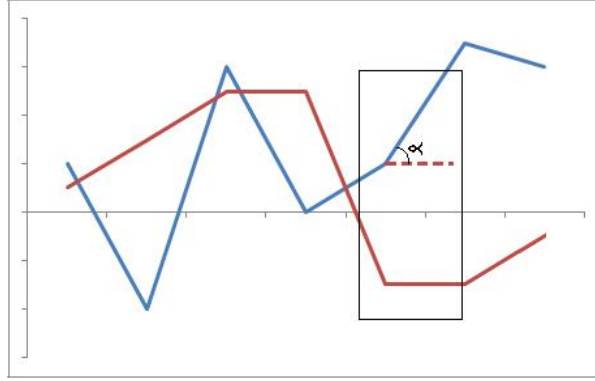
Figure 1: Angles between real vectors.

the most relevant components associated to the different wavelet spectra. We need to measure the distance between the leading patterns, L_x^k and L_y^k, and between the singular vectors, $\mathbf{u}_k$ and $\mathbf{v}_k$. To do so, we compare two vectors by measuring the angle between each pair of corresponding segments. This would be easy to perform if all the values were real (see Figure 1).

In our case, because we use a complex wavelet, we need to define an angle in a complex vector space. Unfortunately, very little guidance is available in the mathematical literature on angles in complex vector spaces and there are several possibilities, Scharnhorst (2001).

Recall that, given two vectors $\mathbf{a}$ and $\mathbf{b}$ in the Euclidian vector space $\mathbb{R}^n$, with the usual inner product $\langle \mathbf{a}, \mathbf{b} \rangle_{\mathbb{R}} = \mathbf{a}^T \mathbf{b}$ and norm $\|\mathbf{a}\| = \sqrt{\langle \mathbf{a}, \mathbf{a} \rangle_{\mathbb{R}}}$, the angle between the two vectors, $\Theta = \Theta(\mathbf{a}, \mathbf{b})$, can be found using the formula:

$$\cos(\Theta) = \frac{\langle \mathbf{a}, \mathbf{b} \rangle_{\mathbb{R}}}{\|\mathbf{a}\| \|\mathbf{b}\|}, \quad \Theta \in [0, \pi]. \tag{18}$$

Now, assume that $\mathbf{a}$ and $\mathbf{b}$ are vectors in the vector space $\mathbb{C}^n$. There are two reasonable approaches to define a (real)-valued angle between $\mathbf{a}$ and $\mathbf{b}$. The first one is to consider the isomorphism

$$\phi : \mathbb{C}^n \longrightarrow \mathbb{R}^{2n}$$

$$\mathbf{a} = (a_1, \ldots, a_n) \mapsto \mathcal{R}(a_1), \mathcal{I}(a_1), \cdots \mathcal{R}(a_n), \mathcal{I}(a_n)$$

17

and simply define the *Euclidean* angle between the complex vectors **a** and **b** as the angle (defined by using formula (18)) between the real vectors $\phi(\mathbf{a})$ and $\phi(\mathbf{b})$.

The other approach is based on the use of the Hermitian inner product $\langle \mathbf{a}, \mathbf{b} \rangle_{\mathbb{C}} = \mathbf{a}^H \mathbf{b}$ and corresponding norm $\|\mathbf{a}\| = \sqrt{\langle \mathbf{a}, \mathbf{a} \rangle_{\mathbb{C}}}$. We can then define the so-called *Hermitian angle* between the complex vectors **a** and **b**, $\Theta_H(\mathbf{a}, \mathbf{b})$, by the formula

$$\cos(\Theta_H) = \frac{|\langle \mathbf{a}, \mathbf{b} \rangle_{\mathbb{C}}|}{\|\mathbf{a}\| \|\mathbf{b}\|}, \quad \Theta_H \in \left[0, \frac{\pi}{2}\right]. \tag{19}$$

The measures are not equal, but they are related; see Scharnhorst (2001) for details. In what follows, we make use of the Hermitian angle.[8]

The distance between the kth leading patterns L_x^k and L_y^k is computed as:

$$d\left(L_x^k, \; L_y^k\right) = \frac{1}{T-1} \sum_{n=1}^{T-1} \Theta_H\left(\mathbf{l}_x^k(n), \; \mathbf{l}_y^k(n)\right), \tag{20}$$

where $\mathbf{l}_x^k(n)$ is the two-component vector defined by the two "points" in $\mathbb{R} \times \mathbb{C}$, $P_n = (n, L_x^k(n))$ and $P_{n+1} = ((n+1), L_x^k(n+1))$, i.e. $\mathbf{l}_x^k(n) = (1, L_x^k(n+1) - L_x^k(n+1))$, where $L_x^k(n)$ denotes the nth component of L_x^k. The distance between the singular vectors, $d\left(\mathbf{u}_k, \mathbf{v}_k\right)$ is defined in an analogous way.

To compare the wavelet spectra of country x and country y, we compute the following distance:

$$\text{dist}\left(W_x, W_y\right) = \frac{\sum_{k=1}^{K} \sigma_k^2 \left[d\left(L_x^k, L_y^k\right) + d\left(\mathbf{u}_k, \mathbf{v}_k\right)\right]}{\sum_{k=1}^{K} \sigma_k^2}, \tag{21}$$

where σ_k^2 are the weights equal to the squared covariance explained by each axis. This distance is computed for each pair of countries. With this information, we can fill a matrix of distances.

---

[8]Using the Euclidian approach angle does not change the results in a sensible way.

3   Business Cycle Synchronism in the Euroland

We analyze the cycles of the core of the Euro area looking both at the frequency content and phasing of cycles. In our analysis we consider the first 12 countries joining the Euro: Austria, Belgium, Finland, France, Germany, Greece, Ireland, Italy, Luxembourg, Netherlands, Portugal and Spain. For this type of purpose, to measure real economic activity, most studies use either real GDP or and Industrial Production Index. We will use the Industrial Production Index because wavelet analysis is quite data demanding, and to have monthly data is a bonus. Using the International Financial Statistics database of the IMF, we gather data from July 1975 until August 2008. To remove short-run noise (frequencies above one year and a half) and long-run trend (frequencies below 9 years), we apply a wavelet-filter (see equation 4).

In Table 1, we can find the countries dissimilarity matrix, based on formula (21) and computed with the whole dataset.

Table 1:   Dissimilarity matrix

	Sp	Pt	Gr	Fi	Ne	Lx	It	Ge	Fr	Be	Au	Ir
Spain	0											
Portugal	0.420	0										
Greece	0.460	0.665	0									
Finland	0.457	0.518	0.386	0								
Netherlands	0.251	0.364	0.470	0.537	0							
Luxembourg	0.270	0.402	0.474	0.555	0.177	0						
Italy	0.342	0.502	0.480	0.384	0.394	0.383	0					
Germany	0.234	0.422	0.413	0.418	0.153	0.175	0.333	0				
France	0.248	0.425	0.424	0.477	0.251	0.266	0.361	0.234	0			
Belgium	0.264	0.334	0.516	0.468	0.245	0.273	0.300	0.224	0.279	0		
Austria	0.269	0.498	0.358	0.315	0.191	0.176	0.360	0.130	0.253	0.293	0	
Ireland	0.303	0.389	0.437	0.341	0.294	0.295	0.343	0.288	0.350	0.242	0.281	0

In this sense, the tighter countries are Germany, Netherlands and Austria. The most dissimilar are Portugal and Greece. Also, if we find the average of the distance between each country and every other country, we see that, on average, the country that is closest to everyone else is Germany, followed by Austria, Netherlands, Belgium, Luxembourg, Spain,
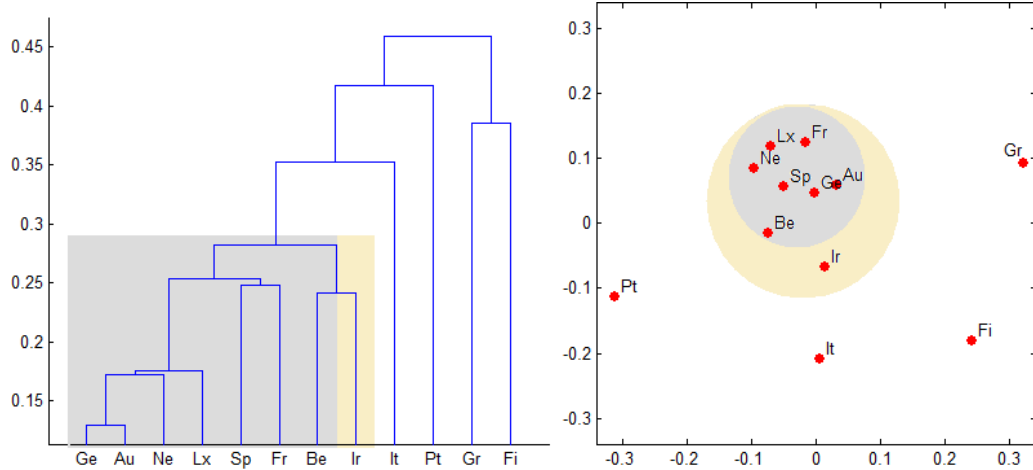
Figure 2: Distance tree, on the left, and multidimensional scaling map, on the right.

Ireland, France, Italy, Finland, Portugal, and Greece. Interestingly, although Luxembourg and Belgium share a common currency since 1944, these two countries are not particularly synchronous. According to Table 1, this pair of is just the 20th most synchronous pair.

To visualize this matrix, we first perform some clustering analysis (e.g. see Camacho *et al.* 2006). First we produce a hierarchical tree clustering. The idea is to group the countries according to their similarities. We follow a bottom up approach. We start with the 12 countries and group, in cluster, the two most similar countries, say C_1 and C_2. In the second round, countries C_1 and C_2 are replaced by a a combination of the two, say C_{13}. Now one has to build a new matrix, not only with the distance between the 10 remaining countries, but also with the distance between each country and C_{13} (which we consider to be the average of the individual distances). The procedure continues until there is only one cluster with all the countries. In Figure 2, on the left, we can see the result of this hierarchical clustering.

From the tree it is clear that there is a core, formed by Germany, Austria, Netherlands, Luxembourg, Spain and France. To this group, we should add Belgium and, maybe, Ireland (from the distance matrix, it is clear that Ireland is further away from the core than Belgium). Although very suggestive, this tree has some limitations that may distort the analysis, because each country is only linked to one other country (or cluster), one may loose site of

the whole picture. We have already mentioned the case of Belgium that is closer to the core than Ireland. Greece is another example. Greece is closer to Austria than to Finland and this cannot be inferred from the tree. An alternative approach is to use the distance matrix to map the countries in a two axis system. This cannot be performed exactly because the distance matrix is not based on euclidean distances. Still, one can reduce the distance matrix to a two column matrix. This new matrix, the configuration matrix, contains the position of each country in two orthogonal axis. Therefore we can put each country on a two dimensional map. The positions in the map are chosen in a way that minimizes the square differences between the distances in the map and the 'true' distances given in Table 1. Figure 2, on the right, shows this map. Again, it is clear that there is an Euroland core, formed by Germany, Austria, the Benelux countries, France, Spain, and, maybe, Ireland.[9] Camacho *et al.* (2006) also concluded that Portugal, Greece and Finland were the countries exhibiting the less "European" cycles. It is comforting to observe that quite radically different approaches do lead to some overlapping results.

Figure 2 gives us a picture of how similar were business cycles in this group of countries since 1975. But it does not tell us how synchronizations have evolved. For example, it is clear that some countries are far away from the Euro core, but nothing is said about their evolution. Are their business cycles becoming more alike or, on the contrary, no convergence is observed? This is the type of analysis that we will try to do next.

3.1   Wavelet Power Spectra

In Figure 3, we can see the continuous wavelet power spectra of the Industrial Production for several countries. To assess the statistical significance, we need to define the null hypothesis. One could use theoretical formulas derived for AR(0) and AR(1) processes. But the assumption that economic time-series follow a white or red noise is quite heroic, therefore we will rely on Monte Carlo simulations. We follow Rouyer *et al.* (2008) and construct the

---

[9]Using the euclidian angles approach, defined in equation 18, the pictures would be similar with one important difference: Ireland would be clearly away from the core. That is why Ireland appears with a different shade.

beta surrogate series The 'beta surrogates' display a similar variance and autocorrelation structure as the original time series and, additionally, display the same relative distribution of frequencies, i.e. the same slope of the Fourier spectrum, as the original time series. With this approach, the surrogate series approximately keep the mean, standard deviation, auto-correlation and partial auto-correlation functions and the power spectrum of the original data.

Looking at the time-scale decomposition interesting facts are revealed. With the exception of Greece, every country shows a spike (white line) around the 6−years frequency. This spike is stronger in the 1980s for several countries (like Ireland, Luxembourg, Germany, Belgium, Netherlands and Austria), while for others, like Portugal and Finland, the high power region is situated between 1990 and 1995). When we look at higher frequencies, around 3−year frequencies, we observe a spike in the 1990s that is common to several countries (although not all of them). The strongest similarity, the six−year spike, which is common to every country, seems independent of the Euro adoption in 1999. Greece starts displaying this same spike slightly before 2000, which may coincide with the strongest efforts of Greece to join the Euro (Greece would eventually join the Euro in 2001).

Although suggestive, the wavelet power spectrum is not the best tool to analyze business cycle synchronization, as no information is revealed about the phase. Therefore, even if two countries share a similar high power region, one cannot infer that their business cycles look alike. To compare countries, cross-wavelet tools are more helpful.

3.2   Phase-difference and cross-wavelets

The phase-difference gives us information on the delay, or synchronization, between oscillations of the two time-series, the cross-wavelet transform will tell us if the correlation is significant or not. To perform the cross-wavelet analysis we will focus on the wavelet coherency, instead of the wavelet cross spectrum, because there is some redundancy between both measures and the wavelet coherency has the advantage of being normalized by the power spectrum of the two time-series. Regions of high coherency between two countries
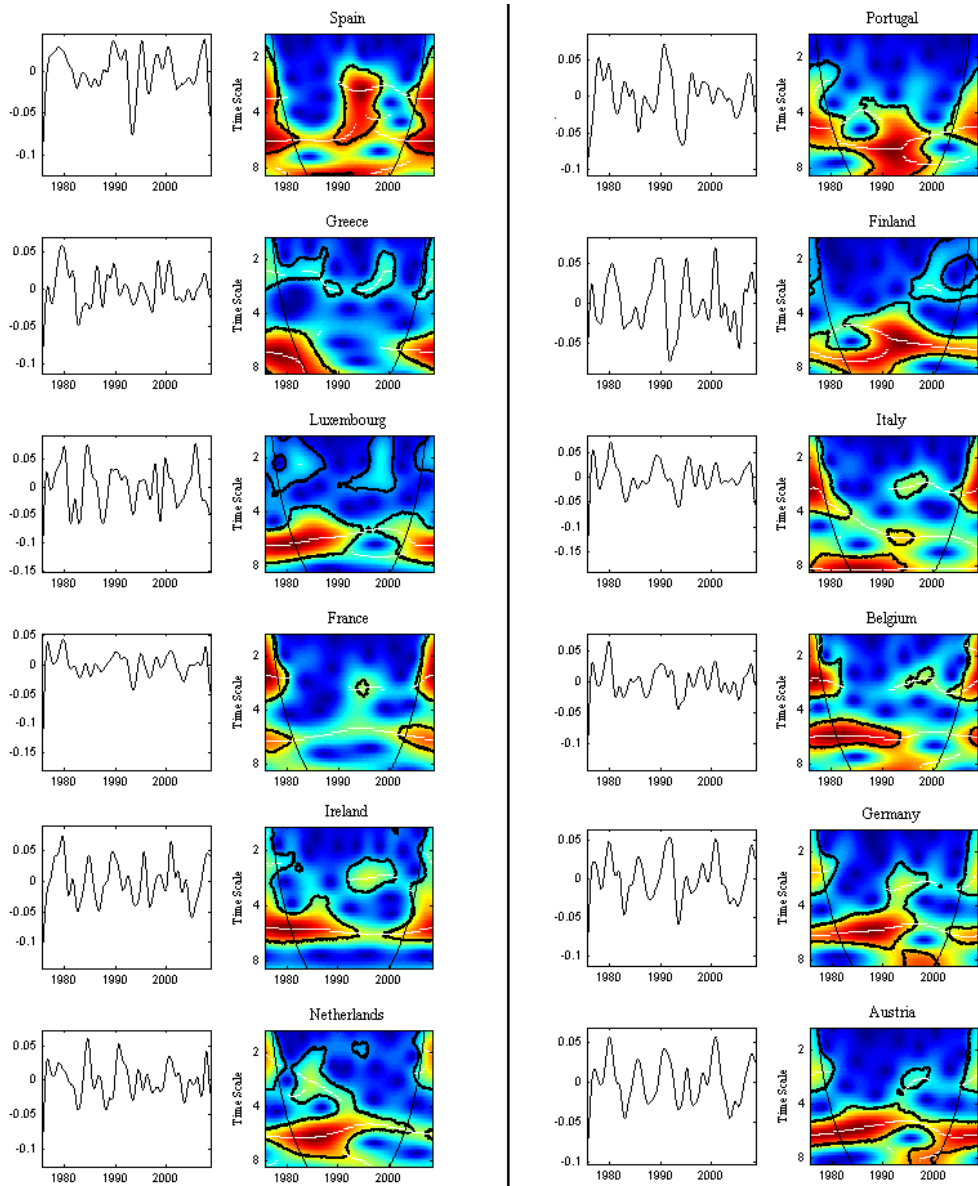
Figure 3: Wavelet Power Spectrum — The black contour designates the 5% significance level estimated by Monte Carlo simulations beta surrogate series. The cone of influence, which indicates the region affected by edge effects, is shown with a thin black line. The color code for power ranges from blue (low power) to red (high power). The white lines show the maxima of the undulations of the wavelet power spectrum.

are synonym of strong local correlation.

In figure 4 we have, on the left, the coherency between German industrial production and the other countries. On the right, we have the phase and an estimate of the instantaneous time lag (equation 14) between the two time-series. On the right we observe two graphs. In the top, the calculations are done between 1.5 and 4.5−year frequencies. In the bottom, we have analysis is performed in the longer run, between 4.5 and 8−year frequencies. Figure 5 gives us the same information but taking France as the reference. We focus on the relations with Germany and France because these are the biggest economies among the countries that formed the Euro core.

Looking at figures 4 and 5, and focusing on the countries that we have identified as the core in Figure 2, we observe that business cycles between Germany and Austria are notably synchronous. The regions of high coherency are very wide, and the phases are very much aligned. These two countries almost behave like one, as we can confirm by noting that the cross-wavelet comparisons between France and Germany are almost indistinguishable from the cross-wavelet comparisons between France and Austria. A similar thing, although not as strong, can be said about Netherlands, although the regions of high coherence are situated at low frequencies. In the case of Belgium, there are several regions of high coherency with Germany both at low frequencies and, specially, at high frequencies. Interestingly, the phases are aligned at high frequencies, but not so much so at low frequencies. Belgium phases are aligned with the French phases. Luxembourg is an interesting case, because not only phases are not aligned at low frequencies but also, at high frequencies, after 1995 the series are consistently unaligned. Still, comparing Luxembourg with France one sees that Luxembourg's accent is more French than German. France and Germany show several regions of high coherency, specially after 1990. The shorter run cycle (higher frequencies) displays similar patterns, but, in the longer run cycle, this is no longer true, and Germany follows France with a lag of about one year. Spain, after 1990, shows regions of strong coherency, specially with France, and the shorter run cycle is aligned both with Germany and France. The longer cycle is similar to the French one. Finally, Ireland does not display
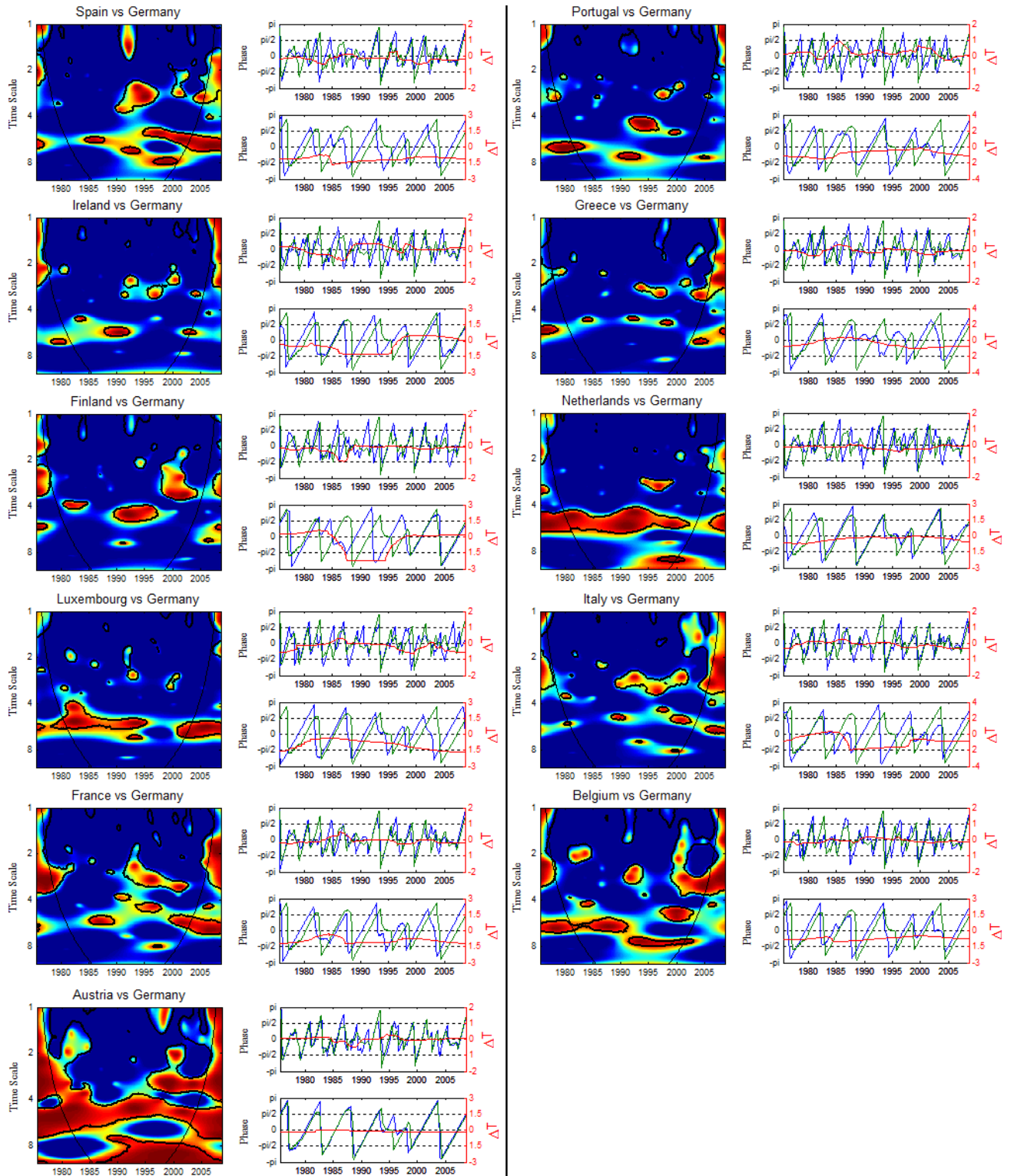
24

Figure 4: On the Left:Cross-Wavelet Coherency − The black thick contour designates the 5% significance level estimated by Monte Carlo simulations using beta surrogate series. The color code for coherency ranges from blue (low coherency – close to zero) to red (high coherency – close to one). On the right: Phase and instantaneous time lag between the two series. The green line represents the German phase, and the blue line represents the other country's phase. The red line gives us the instantaneous time lag between the two series.
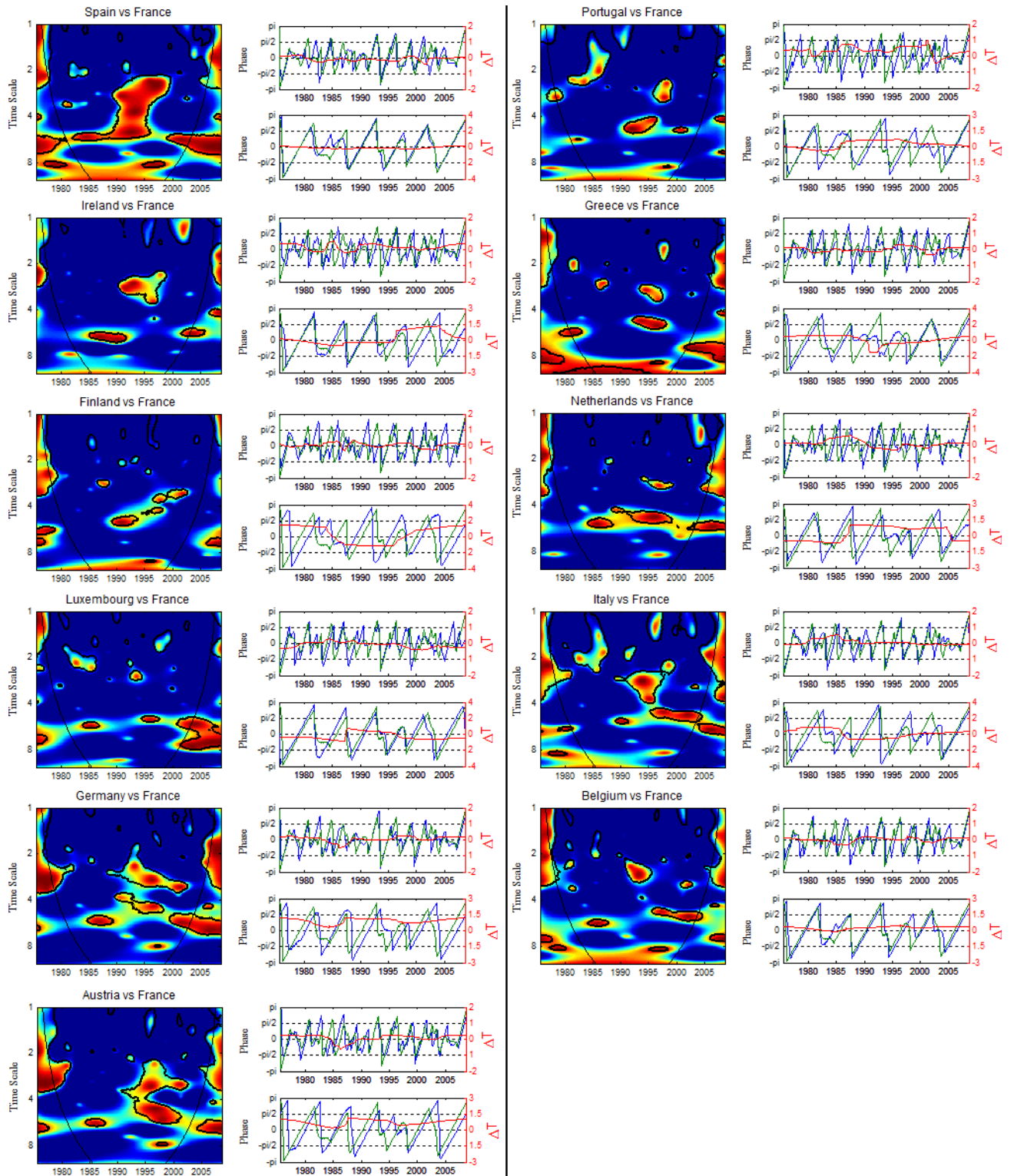
Figure 5: On the Left:Cross-Wavelet Coherency − The black thick contour designates the 5% significance level estimated by Monte Carlo simulations using beta surrogate series. The color code for coherency ranges from blue (low coherency – close to zero) to red (high coherency – close to one). On the right: Phase and instantaneous time lag between the two series. The green line represents the French phase, and the blue line represents the other country's phase. The red line gives us the instantaneous time lag between the two series.

many regions of high coherency, but it is clear that after 1995 the phases are getting more similar to the phases of Germany and France.

With the exception of Portugal, countries that are not in the core, are converging to the core. E.g., although Greece does not display large areas of high coherency, it displays a short-run cycle that after the 1990's is similar to the German cycles. After 1995, its longer run cycle is highly coordinated with the French one. Finland, after 1990, shows some areas of high coherency with Germany, specially at the 5−year scale between 1990 and 1997 and at the 2∼4-year time scale around the year 2000. The shorter-run phase has been quite aligned since 1990 and the longer-run phase clearly converged to the German one. Finally, Italy, specially after the 1990s, shows several regions highly coherent with France, and the short-run cycle is very well aligned with the French one too. It is also clear that after 1995 the longer-run phase is converging to the French one.

4   Conclusions

We have claimed that wavelet analysis can naturally be applied to the study of business cycles (given its periodic nature), specially when one is interested in estimating the spectrum as a function of time, revealing how the different periodic components of the time-series change over time. We used the wavelet spectra to investigate business cycles synchronization in the Euro12 countries. To compare the wavelet spectra we focused on the common high power time-frequency regions, extracting the components of the covariance matrix of the wavelet spectra pairs using the 'Singular Value Decomposition'. Because the wavelet is complex, we had to define the distance between complex vectors, which led us to use the so-called Hermitian angles. Given this, we proposed a metric to measure the distances between wavelet spectra and built a dissimilarity matrix, to which we applied clustering and multidimensional scaling techniques and derived an Euro-core and an Euro-periphery in terms of business cycles synchronism. Using cross wavelet tools, such as wavelet coherency, wavelet phases and wavelet phase-differences, we checked if business cycles of the peripheral countries have became more synchronous with the Euro-core business cycles.

According to our results, Germany, Austria, France, Austria, Spain and the Benelux countries form the Euro-core, while Portugal, Italy, Greece, and Finland are in the periphery. In the Euro-core the two biggest economies are Germany and France, around which the other countries gravitate. The Austrian business cycle is almost indistinguishable from the German one and the same happens, in a lesser degree, with the Netherlands. The Belgium business cycle, and the Spanish after 1990, is aligned with France. We have found some, although not full, support to the argument that countries that share a common currency will see there business cycles becoming more synchronous. With the exception of Portugal, every country not in the Euro-core is converging to the core, This convergence is not homogeneous, though. For example, while the Italian business cycle converges to the French one, Greece displays a short-run cycle that, after the 1990s, is converging to the German cycles and a longer-run cycle that, after 1995 is converging to the French cycle and Finland is converging to the German cycle both at higher and lower frequencies.

References

[1] Aguiar-Conraria, L., Azevedo, N. and Soares, M. J. (2008) "Using Wavelets to Decompose the Time-Frequency Effects of Monetary Policy", *Physica A: Statistical Mechanics and its Applications*, 387, 2863–2878.

[2] Artis, M., Krolzig, H.-M. and Toro, J. (2004) "The European business cycle", *Oxford Economic Papers,* 56, 1–44.

[3] Baxter, M. and Kouparitsas, M. (2005) "Determinants of business cycle comovement: a robust analysis", *Journal of Monetary Economics,* 52, 113–157.

[4] Bloomfield, D., McAteer, R., Lites, B., Judge, P., Mathioudakis, M. and Keena, F. (2004), "Wavelet Phase Coherence Analysis: Application to a Quiet-Sun Magnetic Elelement", *The Astrophysical Journal,* 617, 623–632.

[5] Camacho, M., Perez-Quiros, G. and Saiz, L. (2006) "Are European business cycles close enough to be just one?" *Journal of Economics Dynamics and Control,* 30, 1687–1706.

[6] Camacho, M., Perez-Quiros, G. and Saiz, L. (2008), "Do European Business Cycles Look Like One", *Journal of Economic Dynamics and Control,* 32, 2165-2190.

[7] Cazelles, B., Chavez, M., de Magny, G. C., Guégan, J-F and Hales, S. (2007), "Time-Dependent Spectral Analysis of Epidemiological Time-Series with Wavelets", *Journal of the Royal Society Interface,* 4, 625–36.

[8] Clark, T.E. and Wincoop, E. (2001) "Borders and business cycles", *Journal of International Economics,* 55, 59–85.

[9] Connor, J. and Rossiter, R. (2005), "Wavelet Transforms and Commodity Prices", *Studies in Nonlinear Dynamics & Econometrics,* 9 (1), Article 6.

[10] Crowley, P. (2007), "A Guide to Wavelets for Economists", *Journal of Economic Surveys,* 21 (2), 207–267.

[11] Crowley, P., Maraun, D. and Mayes, D. (2006) "How hard is the euro area core? An evaluation of growth cycles using wavelet analysis", *Bank of Finland Research*, Discussion Papers 18.

[12] Daubechies, I. (1992) *Ten Lectures on Wavelets*, CBMS-NSF Regional Conference Series in Applied Mathematics, vol. 61 SIAM, Philadelphia.

[13] Forni, M., Hallin, M, Lippi, M. and Reichlin, L. (2000) "The Generalized Dynamic-Factor Model: Identification and Estimation", *The Review of Economics and Statistics*, 82, 540-554.

[14] Foufoula-Georgiou, E. and Kumar, P. (1994), *Wavelets in Geophysics*, volume 4 of *Wavelet Analysis and Its Applications*. Academic Press, Boston.

[15] Frankel, J.A. and Rose, A.K. (1998) "The endogeneity of the optimum currency area criteria", *The Economic Journal,* 108, 1009–1025.

[16] Gallegati, M. (2008), "Wavelet analysis of stock returns and aggregate economic activity", *Computational Statistics and Data Analysis*, 52, 3061—3074.

[17] Gallegati, M. and Gallegati, M. (2007), "Wavelet Variance Analysis of Output in G-7 Countries", *Studies in Nonlinear Dynamics & Econometrics*, 11 (3), Article 6.

[18] Gençay, R., Selçuk, F. and Witcher, B. (2005), "Multiscale Systematic Risk", *Journal of International Money and Finance,* 24, 55–70.

[19] Goupillaud, P., A. Grossman and Morlet, J. (1984), "Cycle-Octave and Related Transforms in Seismic Signal Analysis", *Geoexploration*, 23, 85–102.

[20] Grossmann, A. and Morlet, J. (1984), "Decomposition of Hardy Functions into Square Integrable Wavelets of Constant Shape", *SIAM Journal on Mathematical Analysis,* 15, 723-736.

[21] Harding, D. and Pagan, A. (2006) "Synchronization of cycles", *Journal of Econometrics,* 132, 59–79.

[22] Hudgins, L., Friehe, C. and Mayer, M. (1993) "Wavelet Transforms and Atmospheric Turbulence" *Physical Review Letters*, 71:20, 3279-82.

[23] Imbs, J. (2004) "Trade, finance, specialization, and synchronization", *The Review of Economics and Statistics,* 86, 723–734.

[24] Inklaar, R., Jong-A-Pin, R. and de Haan J. (2008) "Trade and business cycle synchronization in OECD countries—A re-examination", *European Economic Review*, 52, 646–666

[25] Kaiser, G. (1994), *A Friendly Guide to Wavelets*, Birkhäuser, Basel.

[26] Raihan, S., Wen, Y. and Zeng, B. (2005), "Wavelet: A New Tool for Business Cycle Analysis", *Working Paper 2005-050A*, Federal Reserve Bank of St. Louis.

[27] Ramsey, J. and Lampart, C. (1998a), "Decomposition of Economic Relationships by Time Scale Using Wavelets: Money and Income", *Macroeconomic Dynamics*, 2, 49–71.

[28] Ramsey, J. and Lampart, C. (1998b), "The Decomposition of Economic Relationships by Time Scale Using Wavelets: Expenditure and Income"**,** *Studies in Nonlinear Dynamics and Econometrics*, 3, 23–42.

[29] Rose, A. and Engel, C., (2002) "Currency unions and international integration", *Journal of Money, Credit and Banking,* 34, 1067–1089.

[30] Rouyer, T., Fromentin, J.-M., Stenseth, N. and Cazelles, B. (2008) "Analysing multiple time series and extending significance testing in wavelet analysis", *Marine Ecology Progress Series*, 359, 11-23.

[31] Scharnhorst, K. (2001) "Angles in Complex Vector Spaces", *Acta Applicandae Mathematicae*, 69, 95–103.

[32] Selover, D. and Jensen, R. (1999) "'Mode-locking' and international business cycle transmission", *Journal of Economic Dynamics and Control,* 23, 591–618.

[33] Torrence, C. and Compo, G. P. (1998), "A Practical Guide to Wavelet Analysis", *Bulletin of the American Meteorological Society*, 79, 605–618.